Electronic Journal of Biotechnology 17 (2014) 55–64

Contents lists available at ScienceDirect

Electronic Journal of Biotechnology

Cyclodextrin glucanotransferase immobilization onto functionalized magnetic double mesoporous core–shell silica nanospheres

Abdelnasser S.S. Ibrahim [a,b,*], Ali A. Al-Salamah [a], Ahmed Mohamed El-Toni [c,d], Mohamed A. El-Tayeb [a], Yahya B. Elbadawi [a]

[a] Department of Botany and Microbiology, College of Science, King Saud University, Riyadh 11451, Saudi Arabia
[b] National Research Center, El-Buhouth St., Dokki, Cairo 12311, Egypt
[c] King Abdullah Institute for Nanotechnology, King Saud University, Riyadh 11451, Saudi Arabia
[d] Central Metallurgical Research and Development Institute, Helwan 11421, Cairo, Egypt

ARTICLE INFO

Article history:
Received 24 September 2013
Accepted 28 November 2013
Available online 28 January 2014

Keywords:
Amphibacillus sp.
Cyclodextrin glucanotransferase
Cyclodextrins
Double mesoporous core–shell silica nanospheres
Immobilization

ABSTRACT

Background: Cyclodextrin glucanotransferase (CGTase) from *Amphibacillus* sp. NPST-10 was covalently immobilized onto amino-functionalized magnetic double mesoporous core–shell silica nanospheres (mag@d-SiO_2@m-SiO_2-NH_2), and the properties of the immobilized enzyme were investigated. The synthesis process of the nanospheres included preparing core magnetic magnetite (Fe_3O_4) nanoparticles, coating the Fe_3O_4 with a dense silica layer, followed by further coating with functionalized or non-functionalized mesoporous silica shell. The structure of the synthesized nanospheres was characterized using TEM, XRD, and FT-IR analyses. CGTase was immobilized onto the functionalized and non-functionalized nanospheres by covalent attachment and physical adsorption.
Results: The results indicated that the enzyme immobilization by covalent attachment onto the activated mag@d-SiO_2@m-SiO_2-NH_2, prepared using anionic surfactant, showed highest immobilization yield (98.1%), loading efficiency (96.2%), and loading capacity 58 μg protein [CGTase]/mg [nanoparticles]) which were among the highest yields reported so far for CGTase. Compared with the free enzyme, the immobilized CGTase demonstrated a shift in the optimal temperature from 50°C to 50–55°C, and showed a significant enhancement in the enzyme thermal stability. The optimum pH values for the activity of the free and immobilized CGTase were pH 8 and pH 8.5, respectively, and there was a significant improvement in pH stability of the immobilized enzyme. Moreover, the immobilized CGTase exhibited good operational stability, retaining 56% of the initial activity after reutilizations of ten successive cycles.
Conclusion: The enhancement of CGTase properties upon immobilization suggested that the applied nano-structured carriers and immobilization protocol are promising approach for industrial bioprocess for production of cyclodextrins using immobilized CGTase.

1. Introduction

Cyclodextrin glycosyltransferases (CGTases) (EC 2.4.1.19) represent one of the most important group of microbial amylolytic enzymes catalyzing four different reactions: cyclization, coupling, disproportionation, and hydrolysis reactions [1,2]. CGTases are used mainly for commercial production of cyclodextrins (CDs) that are produced as a result of intramolecular transglycosylation (cyclization) reaction from degradation of starch and related sugars by CGTase [3]. CDs are of three main types: α-, β-, and γ-cyclodextrin that composed of six, seven, and eight α-(1,4) linked glucose units, respectively [4].

The arrangement of glucose units in a CD molecule results in the shape of a hollow truncated cone with a hydrophilic external surface and a hydrophobic internal cavity which enables CDs to form versatile inclusion complexes with many organic and inorganic substances. Inclusion of the guest compound in CD molecules can lead to favorable changes in chemical and physical properties of the guest molecules [5,6]. Therefore, CDs are mainly used as complexing agents in food, pharmaceutical, and cosmetic industries [3]. Hence, there is increasing interest in developing efficient industrial bioprocesses of CD production for addressing applications in various industries.

* Corresponding author at: Department of Botany and Microbiology, College of Science, King Saud University, Riyadh 11451, Saudi Arabia.
E-mail address: ashebl@ksu.edu.sa (A.S.S. Ibrahim).
Peer review under responsibility of Pontificia Universidad Católica de Valparaíso.

Production and hosting by Elsevier

http://dx.doi.org/10.1016/j.ejbt.2014.01.001

However, biocatalyst stability is of major concern in almost all bioprocesses due to its impact on process cost and economics. Reduced biocatalyst stability results in longer reaction times, lower product yields and increased frequency of catalyst replacement [2]. Enzyme immobilization on solid supports is one of the most useful approaches to overcome such difficulties [7,8]. Application of immobilized enzymes in bioprocesses can offer several advantages over the free enzyme such as improved enzyme stability, reusability of the enzyme, simplifying product purification process, better control of the operation, and providing opportunities for scaling up [9,10]. In this regards, recent advance in nanostructured materials technology has provided a wealth of diverse nanoscaffolds that could potentially support enzymes immobilization [11]. Nanoscale materials provide the upper limits in balancing the key factors that determine the efficiency of biocatalysts, including surface area/volume ratio, mass transfer resistance, and effective enzyme loading [12]. Unlike sol–gel silica, mesoporous silica (MPS) nanoparticles provide tuneable and uniform pore system, functionalizable surfaces, and restricted nanospaces for enzymes immobilization [13]. Moreover, MPS materials show biocompatibility, low cytotoxicity, large surface areas, and easy functionalization that allow enzyme immobilization by various methods including physical adsorption, electrostatic interaction, and covalent attachment [14,15,16]. Moreover, it was recognized that the rigid structure and pore surface of functionalized MPS could mimic protein skeleton where the active sites are held stably with a fixed configuration to carry out the presumed enzymatic functions with good turnover efficiency [15]. Furthermore, the recent developments in silica core/shell structure, consisting of dense silica core coated with mesoporous silica shell, fabrication are responsible for significant progress in technological applications [17].

CGTases have been previously immobilized on traditional macro-carriers, however there are rare, if any, reports about CGTase immobilization on nanostructured materials [2,10,18]. In the present study, CGTase from recently isolated alkaliphilic *Amphibacillus* sp. NPST-10 [19] was immobilized onto magnetic silica core/shell nanospheres. As shown in Fig. 1, the synthesis process of the nanospheres included (i) synthesis of core magnetic magnetite (Fe_3O_4) nanoparticles; (ii) coating of the Fe_3O_4 with dense silica layer; (iii) further coating with functionalized and non-functionalized mesoporous silica shell; and (vi) activation of the functionalized magnetic silica core/shell nanospheres. CGTase was immobilized onto the synthesized magnetic silica core/shell nanospheres by physical adsorption and covalent attachment (Fig. 1). Subsequently, the properties of immobilized enzyme were evaluated compared with the free enzyme.

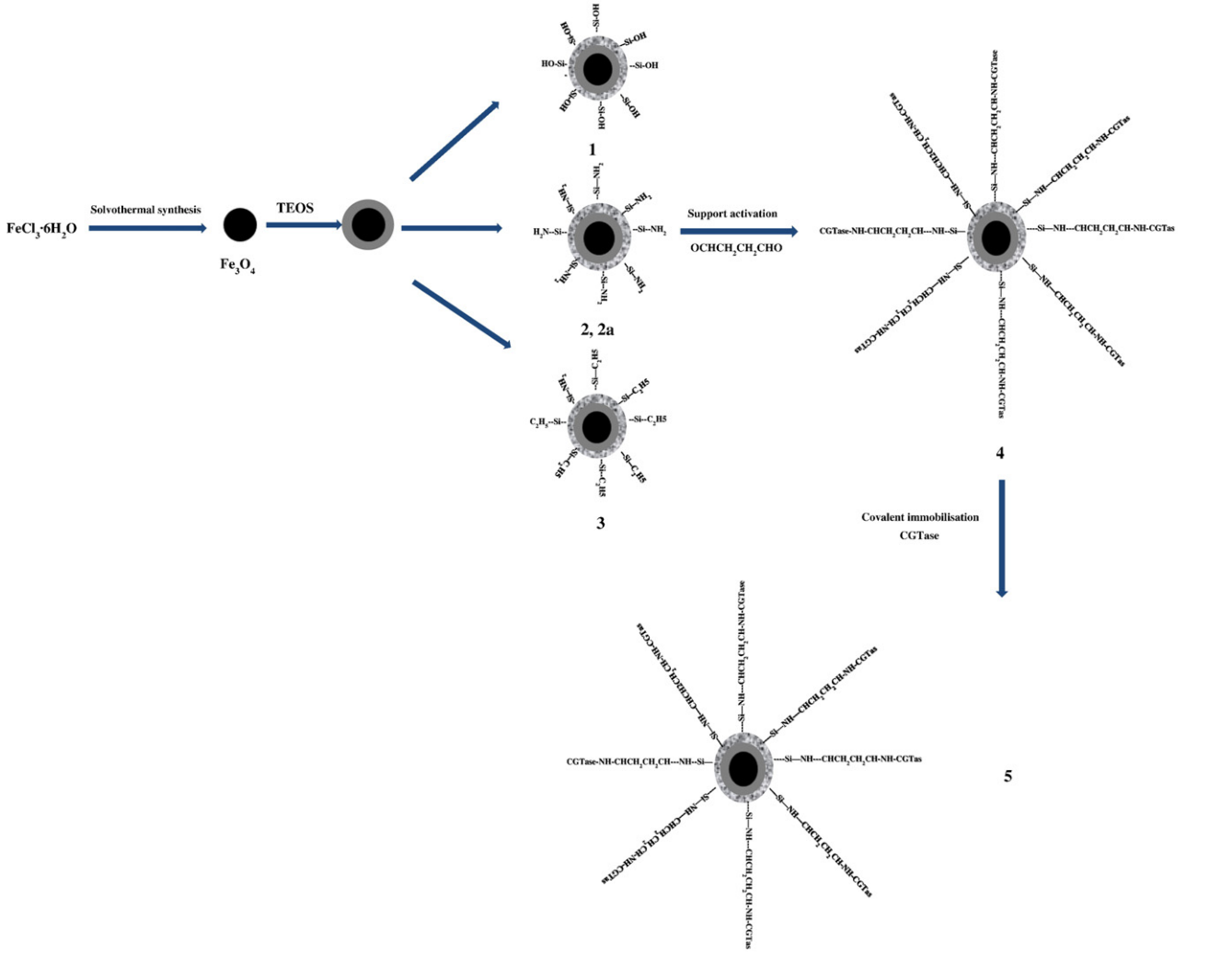

Fig. 1. The scheme used for synthesis of non-functionalized and functionalized magnetic core@dense SiO_2@mesoporous SiO_2 nanospheres followed by support activation and CGTase immobilization. Structure nos. 1, 2, and 3 were used for CGTase immobilization by physical adsorption. Structure no. 1: mag@d-SiO_2@m-SiO_2; nos. 2 and 2a: mag@d-SiO_2@m-SiO_2-NH_2 prepared using anionic or cationic surfactants; no. 3 mag@d-SiO_2@m-SiO_2-C_2H_5; no. 4: Activated mag@d-SiO_2@m-SiO_2-NH_2 using glutaraldehyde as cross linker; and no. 5: covalently immobilized CGTase.

2. Materials and methods

2.1. CGTase production

CGTase producing alkaliphilic *Amphibacillus* sp. NPST-10 used in this study was recently isolated from hypersaline Soda Lakes, located in Wadi Natrun valley in northern Egypt [19]. For CGTase production, colonies of *Amphibacillus* sp. NPST-10 culture was transferred from an agar plate to 500 ml Erlenmeyer flasks containing 100 ml of alkaline production liquid medium, and incubated overnight at 50°C with shaking (150 rpm). This culture was used to inoculate (2.5%, v/v) 1 l Erlenmeyer flask containing 250 ml of the same medium and incubated at the same condition for approximately 36 h. The enzyme production alkaline medium (pH 10) contained soluble starch (15 g/l, Merck), yeast extract (6 g/l, Difco), peptone (6 g/l), NaCl (30 g/l, Sigma), Na_2CO_3 (15 g/l, Merck), $CaCl_2$ (5 mM, Merck), and 300 μl of trace elements solution [19]. At the end of incubation period, cells and insoluble materials were removed by centrifugation at 6000 × *g* for 15 min at 4°C, and cell-free supernatant was used as a source of the crude enzyme.

2.2. CGTase partial purification

Amphibacillus sp. NPST-10 CGTase purification was carried out through adsorption of the crude CGTase to insoluble corn starch (Merck) followed by enzyme elution using β-CD solution [20]. Briefly, corn starch and ammonium sulfate (Sigma) were added to 1 l of cell-free supernatant at final concentrations of 5% (w/v) and 1 M, respectively. The mixture was maintained at 4°C with continuous gentle agitation for 1 h to allow the CGTase binding to the starch. Next, the mixture was centrifuged at 5000 × *g* for 10 min and the starch pellet was washed twice with cold ammonium sulfate solution (1 M) to remove any unbound proteins. The adsorbed CGTase was eluted from the corn starch by incubating the pellet in 200 ml of Tris–HCl buffer (50 mM, pH 8.0, Sigma) containing β-CD (1 mM) for 30 min at 37°C with shaking, followed by centrifugation at 5000 × *g* for 10 min. The elution step was repeated once with 100 ml of the same β-CD solution, and the eluates were pooled (300 ml) and dialyzed (MWCO 12 kDa, Sigma) against the same buffer at 4°C. The eluate was concentrated using an Amicon ultrafiltration membrane kit (10 kDa cut-off membrane, Millipore) and stored at -20°C until use.

2.3. Preparation of magnetic double mesoporous core–shell silica nanospheres

The scheme used for synthesis of non-functionalized and functionalized magnetic double mesoporous core–shell silica (mag core@dense SiO_2@mesoporous SiO_2) nanospheres is shown in Fig. 1, which included (i) synthesis of core magnetic magnetite (Fe_3O_4) nanoparticles; (ii) coating of the Fe_3O_4 with dense silica layer; and (iii) further coating with functionalized and non-functionalized mesoporous silica shell.

2.4. Synthesis of magnetic Fe_3O_4 nanoparticle

The magnetic magnetite (Fe_3O_4) nanoparticles were prepared using the solvothermal synthesis reaction in accordance with Deng et al. [17], with some modifications. Briefly, $FeCl_3 \times 6H_2O$ (1.35 g, 5 mmol) was dissolved in ethylene glycol (40 ml, Sigma) to form a clear solution, followed by the addition of polyethylene glycol (1.0 g, Sigma), and sodium acetate (3.6 g, Merck) as a stabilizing agent. The mixture was stirred vigorously for 30 min and sealed in a Teflon-lined stainless-steel autoclave (50 ml capacity). The autoclave was heated to 190°C for 18 h, allowed to cool to room temperature, and the black products were washed several times with ethanol and dried at 60°C for 6 h.

2.5. Dense silica coating for Fe_3O_4

The magnetic Fe_3O_4 nanoparticles (prepared above) were first coated with dense silica layer to prevent iron oxide cores from leaching into the mother system under any acidic circumstances [17]. Briefly, 3 ml of Fe_3O_4 (0.88 g Fe_3O_4/90 ml ethanol) nanoparticles (~50 nm in diameter) was dispersed in the mixture of ethanol (30 ml), deionized water (2.6 ml), and concentrated ammonia aqueous solution (1.2 ml), followed by the addition of tetraethyl orthosilicate (TEOS, 0.5 ml, Sigma). After stirring at room temperature for 75 min (0.1 ml/15 min), the silica coated Fe_3O_4 nanospheres were separated using an external magnetic field, and washed with ethanol and water.

2.6. Non-functionalized magnetic silica core/shell nanospheres

Non-functionalized magnetic core@dense SiO_2@mesoporous SiO_2 shell (mag@d-SiO_2@m-SiO_2) nanospheres were prepared as follows. In solution A, 0.3 g cetyltrimethylammonium bromide (CTAB, Sigma) was dissolved in 40 ml (1:1 H_2O/ethanol), then 1 ml ammonia solution (28%) was added. In solution B, previous silica coated Fe_3O_4 nanoparticles were dispersed into 90 ml (2:1 H_2O/ethanol) by ultrasonication for 15 min. Thereafter, solution A was added to B with stirring for 10 min, then 0.6 ml TEOS was added drop wisely with stirring for 4 h. After the end of the reaction, nanoparticles were washed twice with ethanol and once with water [17].

2.7. Functionalized magnetic silica core/shell nanospheres

To have amino (NH_2) function group anchored within mesoporous silica shell (mag@d-SiO_2@m-SiO_2-NH_2), 0.2 ml of APMS (3-Aminopropyltriethoxysilane, Sigma) was co-added with TEOS in the reaction described above [20]. After the end of the reaction, the nanoparticles were washed twice with ethanol and once with deionized water. In addition, to investigate the effect of surfactant type that can in turn affect pore size, anionic rather than cationic surfactant has been implemented to construct amino functionalized mesoporous silica shell. Mesoporous silica shell constructed by anionic surfactant usually contains NH_2 groups due the presence of co-structure directing agent (APMS) that assist the electrostatic interaction between negatively charged silica layer and the negatively charged surfactant molecules. NH_2-functionalized magnetic core@dense SiO_2@mesoporous SiO_2 shell (mag@d-SiO_2@m-SiO_2-NH_2) nanoparticles were prepared using anionic surfactant as follows. Previous dense silica coated magnetic nanoparticles were dispersed in 50 ml of H_2O by ultrasonication for 10 min. Thereafter, 0.10 ml of 3-aminopropyltrimethoxysilane, 1.4667 g of N-lauroylsarcosine sodium (acidified solution with 4 ml 0.1 M HCl, Sigma) and 0.6 ml of TEOS were added respectively to the reaction mixture with subsequent stirring for 4 h. After the end of reaction, sample was washed twice with ethanol and once with water.

To have ethane function group (as hydrophobic function group) anchored within mesoporous shell (mag@d-SiO_2@m-SiO_2-C_2H_5), 0.2 ml of 1,2-bis(trimethoxysilyl)ethane (BTME, Sigma) was co-added with TEOS. After the end of the reaction, nanoparticles were washed twice with ethanol and once with deionized water [21].

2.8. Solvent extraction

To maintain the presence of function groups within the silica mesopores, the surfactant molecules were removed by solvent extraction technique [22]. For cationic surfactant (CTAB) based samples, the final powder was dispersed in 60 ml of NH_4NO_3/ethanol solution (6 g/L) and refluxed for 1 h at room temperature. This extraction process was repeated twice. For anionic surfactant based samples, the final powder was dispersed in ammonium acetate (8.01 g) in 100 ml (4:1 ethanol: H_2O) and refluxed at 90°C for 12 h [23].

2.9. Characterisation of the synthesized nanoparticles

The transmission electron microscopy (TEM) images of the functionalized and non-functionalized magnetic silica core/shell nanospheres were obtained using a JEOL JSM-2100F electron microscope (Japan) operated at 200 kV. The powder X-ray diffraction (XRD) patterns of the nanoparticles were recorded on a PANalytical X'Pert PRO MPD (Netherlands) with Ni-filtered Cu Kα radiation (45 kV, 40 mA). The nitrogen sorption isotherms were measured at 77 K with a Quantachrome NOVA 4200 analyser (USA). The Brunauer–Emmett–Teller (BET) method was utilized to calculate the specific surface of the nanoparticle areas using adsorption data at the relative pressure range from 0.02 to 0.20. By using the Barrett–Joyner–Halenda (BJH) model, the pore volumes and size distributions of the nanoparticles were derived from the adsorption branches of isotherms, and the total pore volumes (Vt) were estimated from the adsorbed amount at a relative pressure P/P_0 of 0.995. The Fourier transform infrared (FT-IR) spectra were recorded using a Bruker Vertex-80 spectrometer. Magnetic characterization of nanoparticles was carried out on a superconducting quantum interference device (SQUID) magnetometer.

2.10. CGTase immobilization

The partially purified *Amphibacillus* sp. NPST-10 CGTase was immobilized onto the synthesized non-functionalized and functionalized magnetic double mesoporous core–shell silica nanospheres by physical adsorption and covalent attachment (Fig. 1).

2.11. Physical adsorption

Four materials (numbers 1, 2, 2a, 3), without any activation, were used for CGTase immobilization by physical adsorption including: mag@d-SiO_2@m-SiO_2 (Fig. 1, no. 1), mag@d-SiO_2@m-SiO_2-NH_2 prepared using anionic or cationic surfactants (Fig. 1, no. 2), and mag@d-SiO_2@m-SiO_2-C_2H_5 (Fig. 1, no. 3). Briefly, 50 mg of various nanoparticles was suspended in 1 ml of 50 mM glycine buffer (pH 8) containing the purified CGTase, and maintained overnight at 4°C with gentle shaking. The CGTase bound to various nanoparticles was recovered by magnetic separation, washed twice with glycine buffer (50 mM, pH 8) to remove the unbound CGTase, and the washed solution was collected [24,25].

2.12. Covalent attachment

The purified CGTase was covalently immobilized onto the amino functionalized silica coated magnetic nanoparticles (mag@d-SiO_2@m-SiO_2-NH_2), prepared using either anionic or cationic surfactant. First, the support (Fig. 1, no. 2) was activated by glutaraldehyde ($OCHCH_2CH_2CHO$) as bifunctional cross linker agent, followed by coupling of partially purified CGTase to the activated nanoparticles (Fig. 1), [6,20,26]. Briefly, 50 mg of magnetic support was suspended in 10 ml of glutaraldehyde solution (2%, v/v, Sigma), prepared in distilled water, and the mixture was incubated for 2 h at room temperature with stirring. Then, the activated support was collected from the solution using an external magnetic field, and rinsed several times with distilled water to remove the excess glutaraldehyde. Thereafter, the activated nanoparticles were re-suspended in 1 ml of 50 mM glycine buffer (pH 8) containing the purified CGTase and maintained overnight at 4°C with gentle shaking. CGTase bound nanoparticles were recovered by magnetic separation, and washed twice with glycine buffer (50 mM, pH 8) to remove the unbound CGTase, and the washed solution was collected.

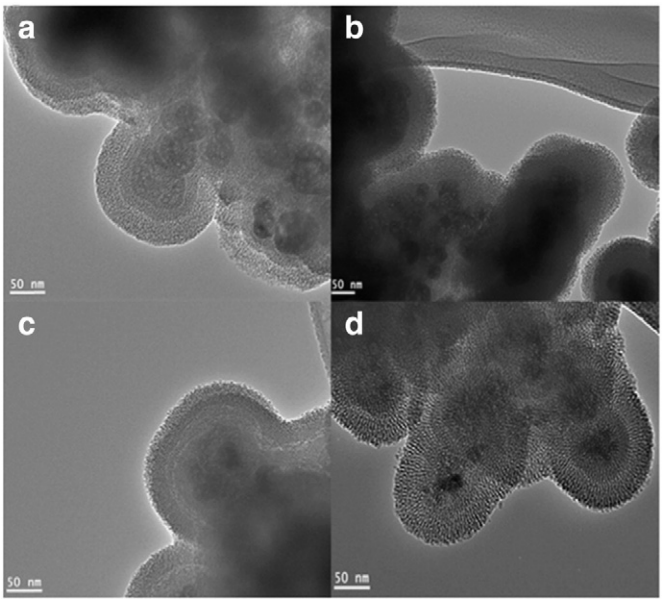

Fig. 2. TEM images of mesoporous silica coated magnetic core@dense SiO_2 (mag@d-SiO_2@m-SiO_2) prepared with cationic surfactant functionalized with (a) no group, (b) NH_2, (c) ethane group and (d) prepared with anionic surfactant functionalized with NH_2.

2.13. Immobilization yield and efficiency

The amount of protein in the free enzyme and washed solution was determined using Bradford method using bovine serum albumin a standard protein [27]. The amount of immobilized CGTase on the nanoparticles was calculated by subtracting the amount protein recovered in the supernatant (washed solution) from the amount of protein subjected to immobilization. The loading efficiency was calculated according to the following equation [26]: loading efficiency = $[(P_i - P_{unb}) / P_i] \times 100$, where P_i and P_{unb} are the initial protein subjected to immobilization, and the unbound protein, respectively. The CGTase activity of the free enzyme, immobilized enzyme, and unbound enzyme was measured as described below. Immobilization and activity yields were calculated according to the following equations: immobilization yield (%) = $[(A - B) / A] \times 100$, where A is the total activity of the enzyme added in the initial immobilization solution and B is the activity of the unbound CGTase. Activity yield = $(C / A) \times 100$, where A is the total activity of the enzyme added in the initial immobilization solution, and C is activity of the immobilized CGTase [26].

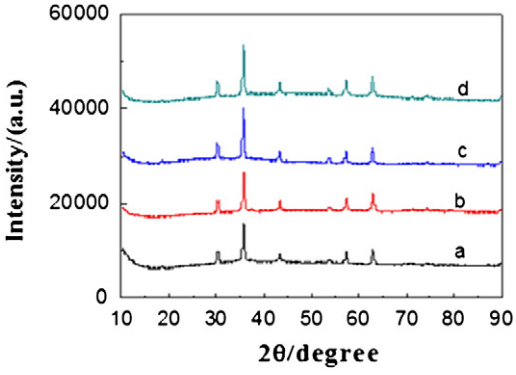

Fig. 3. X-ray diffraction of mesoporous silica coated magnetic core@dense SiO_2 (mag@d-SiO_2@m-SiO_2) prepared with cationic surfactant functionalized with (a) no group, (b) NH_2, (c) ethane group and (d) prepared with anionic surfactant functionalized with NH_2.

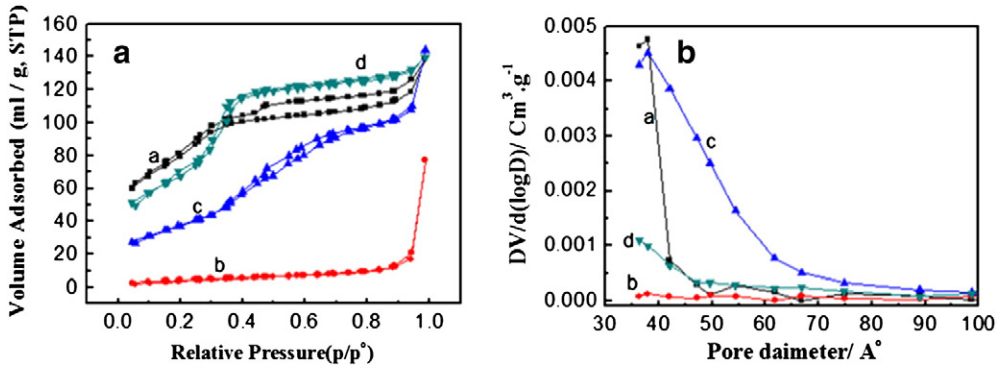

Fig. 4. (a) N_2 adsorption-desorption isotherms and (b) pore size distribution of mesoporous silica coated magnetic core@dense SiO_2 (mag@d-SiO_2@m-SiO_2) prepared with cationic surfactant functionalized with 'a' no group; 'b' NH_2; 'c' ethane group; and 'd' prepared with anionic surfactant functionalized with NH_2.

2.14. Assay of CGTase activity

The CGTase activity of the free and immobilized enzyme was measured as the β-CD forming activity in accordance with previously described methods [19,28], with some modifications. Briefly, 1.5 ml of 1% (w/v) starch solution prepared in glycine buffer (50 mM, pH 8) was pre-incubated at 50°C for 5 min. Next, 200 μl of the free enzyme samples or 50 mg of immobilized CGTase was added to the reaction mixture and after incubating for 20 min at 50°C, the reaction was quenched by the addition of 750 μl of 0.15 M NaOH. Subsequently, 200 μl of 0.02% (w/v) phenolphthalein solution prepared in 5 mM Na_2CO_3 was added, maintained at room temperature for 15 min, and the color intensity was measured at 550 nm. A unit of CGTase activity was defined as the amount of enzyme releasing 1 μM of β-CD per min under the defined assay conditions. A calibration curve was generated using 0.001–0.5 μM of β-CD prepared in 50 mM glycine buffer (pH 8).

2.15. Properties of the immobilized CGTase

2.15.1. Effect of temperature

The effect of temperature on activity of the free and immobilized CGTase was determined by measuring the enzyme activity at various temperatures ranging from 30°C to 75°C under standard assay conditions. For determination of the CGTase thermal stability, the free and immobilized enzymes prepared in 50 mM glycine buffer (pH 8) were incubated at different temperatures (35–75°C) for 1 h in a shaking water bath. Then, the reaction mixtures were cooled immediately in an ice bath, and the residual enzyme activities were determined under the standard assay conditions. The residual activity of the free and immobilized CGTase was calculated and compared with the untreated samples. All experiments and enzyme assays were performed in triplicate and the mean values were recorded.

2.15.2. Effect of pH

The influence of pH on the CGTase activity was established by the determination of the activity of the free and immobilized CGTase at various pH using suitable buffers including 50 mM sodium acetate (pH 5.0 and 6.0), 50 mM Tris–HCl (pH 7.0 and 8.0), 50 mM glycine–NaOH buffer (9.0 and 10.0) and 50 mM carbonate–bicarbonate buffer (pH 11.0 and 12.0). Furthermore, the pH stability of the free and immobilized CGTase was investigated by incubating the enzyme samples in buffers at the different pH for 3 h at room temperature, and the residual activity of the enzymes was assayed under standard assay conditions. All experiments and enzyme assays were performed in triplicate and the mean values were reported.

2.15.3. Operational stability

The operational stability of the immobilized CGTase was evaluated in successive batches using 2 ml of the standard assay mixture. The reaction mixture containing the immobilized was incubated in a shaking water bath (120 rpm) and 45°C for 20 min. At the end of each batch, immobilized enzyme was separated from the reaction mixture using an external magnetic field, washed with glycine buffer (50 mM, pH 8), to remove any substrate or products remaining in the nanoparticles, and resuspended in a freshly prepared substrate solution to restart a new cycle. The activity was estimated at the end of each cycle as described above, and the residual activity was calculated and expressed relative to the initial CGTase activity.

Table 1
Textural properties of magnetic core@ dense SiO_2@ mesoporous SiO_2 shell nanoparticles with different functionalizations.

Sample code	Total pore volume ($cm^3 \cdot g^{-1}$)	Surface area ($cm^2 \cdot g^{-1}$)	Shell thickness (nm)
mag@d-Si@m-SiO_2	0.2148	293.5	33
mag@d-Si@m-SiO_2-NH_2 (cationic)	0.1193	16.280	12
mag@d-Si@m-SiO_2-C_2H_5	0.2229	137.95	33
mag@d-Si@m-SiO_2-NH_2 (anionic)	0.2167	259.62	31

3. Results and discussion

3.1. Characterization of magnetic double mesoporous core–shell silica nanospheres

Magnetite (Fe_3O_4) nanoparticles were first prepared by the solvothermal synthesis reaction. Then, to fabricate functionalized mesoporous silica shell onto magnetic Fe_3O_4 nanoparticle, first Fe_3O_4 was coated with a thin dense silica layer of desired thickness, in order to protect the iron oxide core from leaching into the mother system

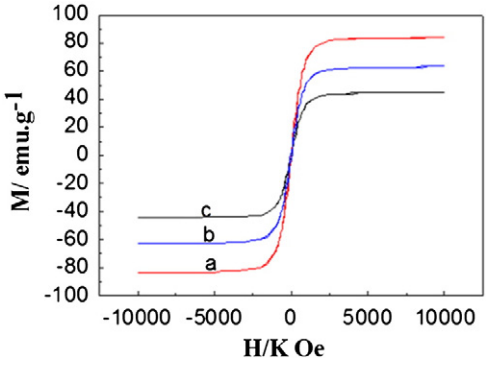

Fig. 5. Room-temperature magnetization curve for (a) Fe_3O_4 and (b) silica coated Fe_3O_4 and (c) mesoporous silica coated magnetic core@dense SiO_2 functionalized with NH_2.

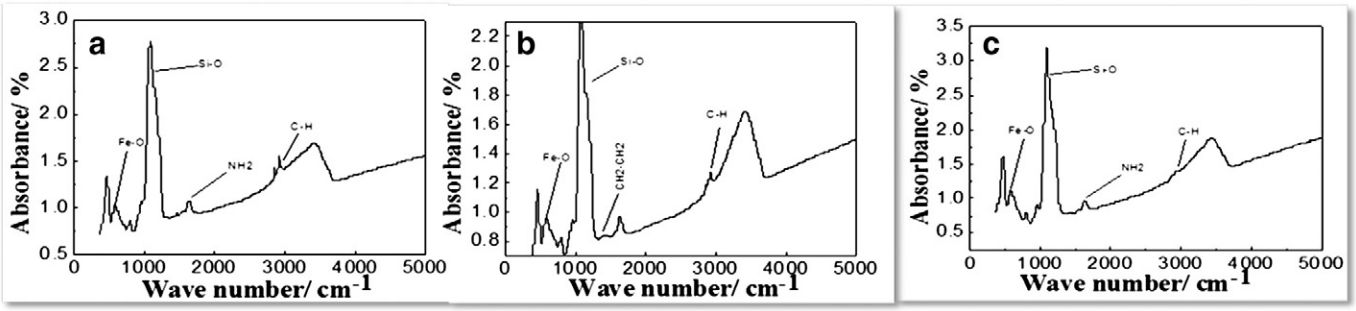

Fig. 6. FT-IR spectra for mesoporous silica coated magnetic core@ dense SiO_2 prepared with cationic surfactant functionalized with (a) NH_2, (b) ethane group and (c) prepared with anionic surfactant functionalized with NH_2 extracted from the adsorption branch.

under any acidic circumstances, followed by synthesis of the functionalized and non-functionalized mesoporous silica layer. TEM images of mag@d-SiO_2@m-SiO_2 with different functionalizations are shown in Fig. 2. It is clear that magnetic dense/mesoporous core–shell structures were developed. Magnetic nanoparticles (dark nanoparticles) can be seen coated with two layers, the first layer is the dense silica layer surrounding the Fe_3O_4 nanoparticles. The second layer is mesoporous silica that functionalized with (a) no group, (b) NH_2, synthesized using cationic surfactant, (c) ethane group, and (d) NH_2, synthesized using anionic surfactant, where the mesoporous shell thicknesses were 33, 12, 33 and 31 nm, respectively. The X-ray diffraction patterns of mag@d-SiO_2@m-SiO_2 with different functionalizations are shown in Fig. 3. All peaks were well indexed as spinel magnetite which are in good agreement with the standard literature data (JCPDF card number: 86-1354) [29]. These sharp diffraction peaks clearly revealed that the spinel magnetite product is well defined crystallites. In addition, no impurity diffraction peaks were detected, suggesting the pure phase of the synthesized magnetite nanoparticles. After different functionalizations of mesoporous silica shell, the XRD patterns exhibited similar diffraction peaks that do not undergo any notable change, suggesting that the magnetite structure was retained [29].

Nitrogen adsorption/desorption isotherms measured at 77 K for the calcined mag@d-SiO_2@m-SiO_2 samples with different function groups are shown in Fig. 4a. The isotherms exhibited the type IV curves, which are characteristic of uniform mesoporous materials [22,23]. The textural properties, total surface area (according to BET theory), and total pore volume of mag@d-SiO_2@m-SiO_2 were superior in case of cationic surfactant without function group and anionic one (Fig. 4a). As shown in Table 1, functionalization of mesoporous silica layer with ethane group caused significant reduction of its surface area, which can be attributed to existence of anchored ethane group that caused some blockage of its surface area. Furthermore, functionalization with NH_2 groups using APMS resulted in pronounced loss of both surface area and porosity. Addition of basic APTES caused an increase of the pH value, that speed up the hydrolysis–condensation rates of alkoxysilane that caused the formation of secondary silica nuclei instead of primary mesoporous silica shell that finally lead to formation of porous shell with low thickness (12 nm), [30]. On the other hand, pore size distribution analysis (Fig. 4b) showed narrow distribution with pore radius around 3.8 nm upon synthesizing mag@d-SiO_2@m-SiO_2 with CTAB and without any functionalization. Upon surface functionalization using APMS, it was clear that pore size centered on 3.8 nm with reduction of the porosity due to suppression of silica shell thickness (12 nm). Implementation of BTME to impart hydrophobicity to mesoporous shell by anchoring ethane groups caused the pore size to be quite broad that indicate the presence of some bigger pores together with main pore size of 3.8. Finally, using anionic surfactant resulted in formation of narrow pore size distribution that was centered on 3.6 nm (Fig. 4b).

The magnetic properties of Fe_3O_4 samples were measured on the superconducting quantum interference device (SQUID) magnetometer. As shown in Fig. 5, the magnetic saturation value for non-coated Fe_3O_4 is 83 emu/g. After dense silica coating process, the magnetite saturation decreased to 60 emu/g. Further decrease in the magnetization saturation to 43 emu/g was noticed after functionalized mesoporous shell formation. The gradual loss of magnetization strength with dense and mesoporous shell formation step can be attributed to shielding effectof silica layer [31]. However, it had no significant effect on the magnetic separability of the nanoparticles from the bulk solution.

Furthermore, FT-IR measurements have been conducted to confirm silica coating for Fe_3O_4 and functionalization of mesoporous silica coated Fe_3O_4. As shown in Fig. 6, Fe_3O_4 nanoparticles showed a strong absorption bands at 580 cm^{-1} that corresponds to Fe – O vibrations of the magnetite core [32]. Upon silica coating of Fe_3O_4, Si–O peak can be seen formed at 1050–1250 cm^{-1}. The Fe–O–Si peak that refer for chemical binding between Fe_3O_4 and silica, cannot be seen in the FT-IR spectrum because it appears at around 584 cm^{-1} and therefore overlaps with the Fe – O vibration of magnetite nanoparticles [32]. However, the co-existence of peaks characteristics for Fe_3O_4 and silica together indicates the silica coating for Fe_3O_4 [33]. On the other hand, APMS functionalization for magnetic core@dense SiO_2@mesoporous SiO_2 can be elucidated from the existence of N–H peak at 1637 cm^{-1}. Moreover, OCH_2CH_3 and C – H stretching vibrations peaks that appeared at 2930 and 2862 cm^{-1} provide further evidence for APMS functionalization of magnetic core@dense SiO_2@mesoporous SiO_2 [33].

Table 2
CGTase immobilization on various magnetic double mesoporous core–shell silica nanospheres by physical adsorption or covalent attachment.

Materials	Immobilization method	Immobilization yield (%)	Activity yield (%)	Loading efficiency (%)
mag@d-Si@m-SiO_2	Physical adsorption	4.4	0.8	6.6
mag@d-Si@m-SiO_2-NH_2 (cationic)	Physical adsorption	19.3	18.2	20.1
mag@d-Si@m-SiO_2-C_2H_5	Physical adsorption	5.9	4.0	5.2
mag@d-Si@m-SiO_2-NH_2 (anionic)	Physical adsorption	45.2	37.6	42.5
Activated mag@d-Si@m-SiO_2-NH_2 (cationic)	Covalent attachment	42.2	36.8	32.3
Activated mag@d-Si@m-SiO_2-NH_2 (anionic)	Covalent attachment	98.1	96.5	92.2

Upon functionalization with hydrophobic moiety (ethane group) using 1,2-bis(trimethoxysilyl)ethane (BTME), the ethane group can be seen at 1415 cm^{-1} (Fig. 6b), indicating their presence within mesoporous silica shell [22]. Furthermore, upon mesoporous shell synthesis using anionic surfactant that contains NH_2 group due to the usage of APMS as co-structure directing agent resulted in the appearance of N–H peak at 1637 cm^{-1} together with some remaining OCH_2CH_3 and C – H stretching vibrations peaks that appeared at 2930 and 2862 cm^{-1} from APMS.

3.2. CGTase immobilization

Immobilization of CGTase onto the synthesized magnetic double mesoporous core–shell silica nanospheres (mag@d-SiO_2@m-SiO_2) was performed by two different methods: physical adsorption and covalent attachment. Enzyme immobilization by physical adsorption was carried out using four synthesized magnetic double mesoporous core–shell silica nanospheres, without any activation, including mag@d-SiO_2@m-SiO_2 (Fig. 1, no. 1), mag@d-SiO_2@m-SiO_2-NH_2 prepared using anionic or cationic surfactants (Fig. 1, no. 2), and mag@d-SiO_2@m-SiO_2-C_2H_5 (Fig. 1, no. 3). To induce CGTase immobilization by covalent attachment to amino functionalized double mesoporous core–shell silica nanoparticles, the free amino groups (– NH_2) lying within the silica shell was further activated by glutaraldehyde as a bifunctional crosslinker (Fig. 1, no. 2). In which, the free amino groups of mag@d-Si@m-SiO_2-NH_2 reacts with terminal aldehyde groups of glutaraldehyde to form a Schiff-base linkage and provides a free terminal aldehyde, which can be then condensed with free amino groups in CGTase molecule to form a second Schiff-base [20,34,35,36].

The results shown in Table 2 indicated that *Amphibacillus* sp. NPST-10 CGTase was successfully immobilized on various magnetic double mesoporous core–shell silica nanospheres, either by physical adsorption or covalent attachment. However, CGTase immobilization by covalent attachment showed higher immobilization yield and loading efficiency compared to enzyme immobilization by physical adsorption. CGTase adsorption onto the hydrophobic mag@d-SiO_2@m-SiO_2-C_2H_5 nanospheres showed the lowest immobilization yield (5.9%) and loading efficiency (5.2%), suggesting the low hydrophobicity of CGTase molecule [24]. In addition, the low immobilization yield of CGTase onto mag@d-SiO_2@m-SiO_2 and mag@d-Si@m-SiO_2-NH_2 by physical adsorption is mostly attributed to low electrostatic interaction between the enzyme and these materials [15]. mag@d-SiO_2@m-SiO_2-NH_2 prepared using anionic surfactant was

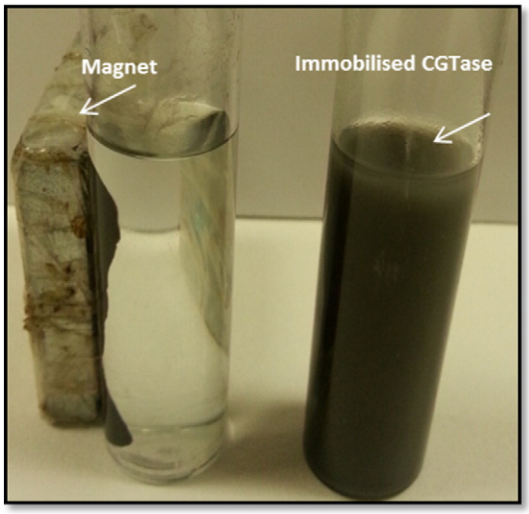

Fig. 7. Magnetic separation of CGTase covalently immobilized on mag@d-Si@m-SiO_2-NH_2 using an external magnetic field.

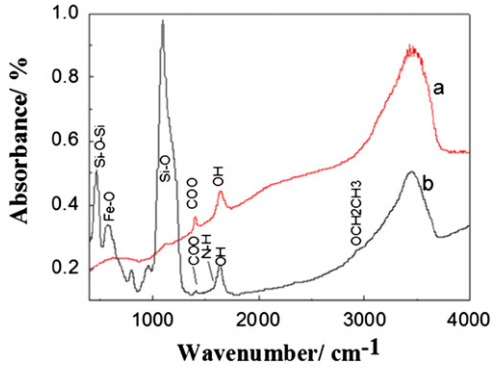

Fig. 8. FTIR spectra of (a) Free CGTase enzyme, and (b) CGTase immobilized on activated mag@d-Si@m-SiO_2-NH_2.

superior for CGTase immobilization compared to that prepared using cationic surfactant, with immobilization yield of 98.1% and 42.2%; and loading efficiency of 96.2% and 75.5%, respectively (Table 2). This can be attributed to the higher shell thickness (31 nm) and surface area (259.62 cm^2 g^{-1}) of mag@d-SiO_2@m-SiO_2-NH_2 prepared using anionic surfactant compared to that prepared using cationic surfactant that showed less shell thickness and surface area of 12 nm and 16.280 cm^2 g^{-1}, respectively (Table 1). Which in turn resulted in higher amino groups available for CGTase in SiO_2@m-SiO_2-NH_2 prepared using anionic surfactant than that prepared using cationic surfactant.

CGTase immobilized by physical adsorption, either by weak hydrophobic or by electrostatic interactions can be easily washed out from the carrier and hence resulted in low immobilization yield and loading efficiency [15,24]. However, when CGTase molecule was immobilized on to the activated carrier by covalent bond, it was strongly attached to the support through glutaraldehyde as cross linker, and hence showed higher immobilization yield and loading efficiency. Thus, the covalent attachment was more effective for *Amphibacillus* sp. NPST-10 CGTase immobilization onto magnetic functionalized double mesoporous core-shell silica nanospheres than physical adsorption and was used for further investigation. As shown in Fig. 7, CGTase immobilized on activated mag@d-Si@m-SiO_2-NH_2 could be easily separated from the bulk solution using an external magnetic field that allows convenient separation for reusing of the immobilized enzyme in bioprocess for cyclodextrins production.

FT-IR measurements have been conducted to confirm the immobilization of CGTase on the surface of mag@d-Si@m-SiO_2-NH_2 (Fig. 8). CGTase enzyme has characteristic peaks at 1400 cm^{-1} for carboxylic (COO) bond [37] and another peak at 1640 cm^{-1} that it could be either NH or OH bond. The binding of enzyme (CGTase) to magnetic core–mesoporous shell nanoparticles prepared using anionic and cationic surfactant was confirmed from the appearance

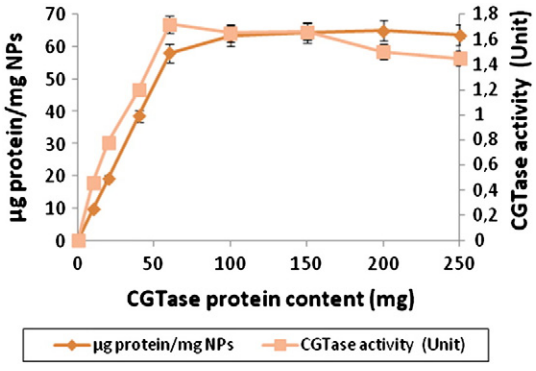

Fig. 9. Effect of the initial amount of CGTase on the binding and activity of immobilized enzyme. Results represent the mean of three separate experiments, and error bars are indicated.

of carboxylic COO bond, characteristic for enzyme, together with these characteristics for amino functionalized magnetic core-mesoporous shell nanoparticles.

3.3. Loading efficiency of the mag@d-SiO_2@m-SiO_2-NH_2 nanoparticles

The loading efficiency of amino functionalized double mesoporous core–shell silica nanospheres (mag@d-SiO_2@m-SiO_2-NH_2), prepared using anionic surfactant, was determined by immobilization of different amounts of CGTase ranged from 1000 to 2500 μg protein onto 10 mg of activated nanospheres. The results illustrated in Fig. 9 showed that the amount of the loaded enzyme increased with increasing the initial CGTase amount showing maximum value of 58 μg protein/mg carrier, and remained constant even by increasing of the enzyme amount up to 250 μg/mg carrier. This loading capacity of CGTase on activated mag@d-SiO_2@m-SiO_2-NH_2 nanospheres is one of the highest values obtained for CGTase immobilization so far [10,26,38,39]. On the other hand, as shown in Fig. 9 the total activity of the immobilized enzyme was increased with increasing of the CGTase up to 60 μg of protein content. Further increase of enzyme concentration led to slight decrease in total activity of the immobilized CGTase, which is likely owing to steric hindrance of CGTase molecules in the silica surface [26,39]. The high immobilization yield, loading efficiency, activity yield of the activated mag@d-SiO_2@m-SiO_2-NH_2 is mostly due to high surface area of the nanospheres (16.28 $cm^2\ g^{-1}$) available for enzyme attachment, and amino functionalization of silica shell using in situ functionalization rather than post synthesis process, which led to incorporation of higher density of free amino groups available for activation and subsequently enzyme immobilization [17,20,40].

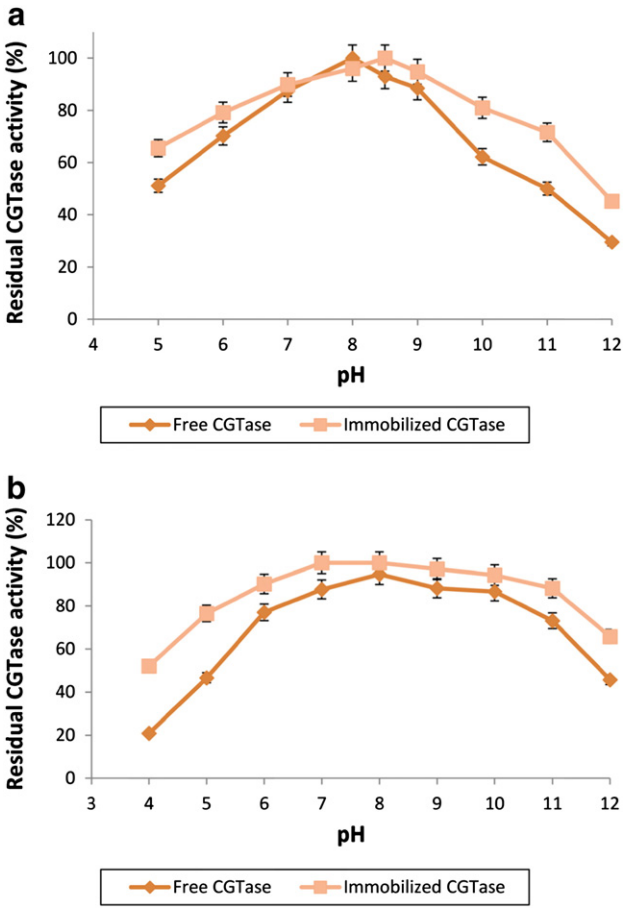

Fig. 10. Effect of pH on the activity (a) and stability (b) of free and immobilized CGTase. Results represent the mean of three separate experiments, and error bars are indicated.

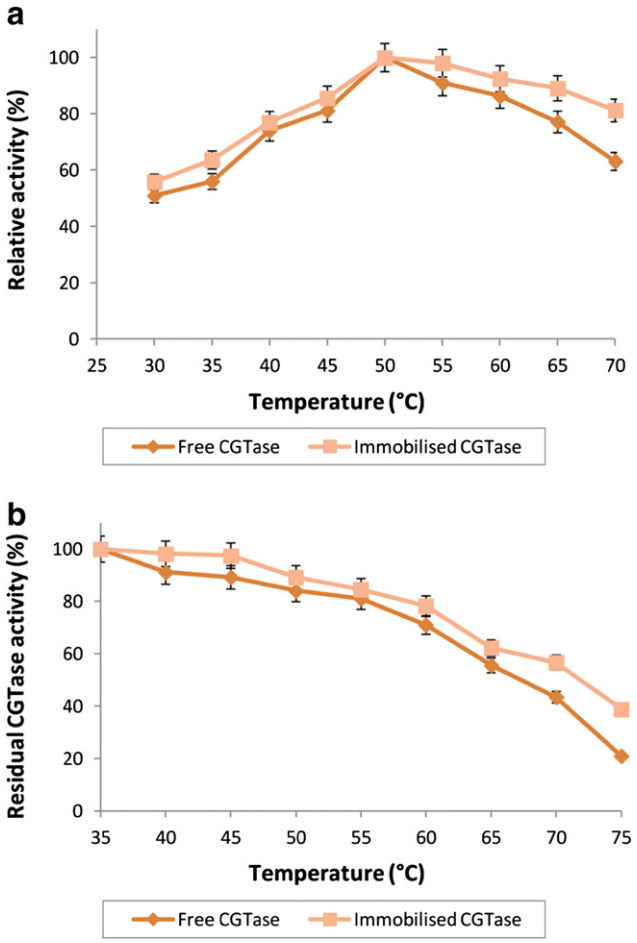

Fig. 11. Effect of temperature on the activity (a) and stability (b) of free and immobilized CGTase. Results represent the mean of three separate experiments, and error bars are indicated.

3.4. Properties of the immobilized CGTase

3.4.1. Effect of pH

The optimum pH for the free and immobilized CGTase was determined by measurement of the enzyme activity at varying pH values ranging from pH 5.0 to 12.0 at 50°C, under the standard assay conditions. As shown in Fig. 10a, the optimum pH of the immobilized CGTase was shifted from pH 8 for free CGTase to pH 8.5 for immobilized enzyme. In addition, a significant increase of the relative activity of the immobilized CGTase compared to free enzyme was observed, particularly at high pH values. Generally, the optimum pH value of an immobilized enzyme can shift to a higher

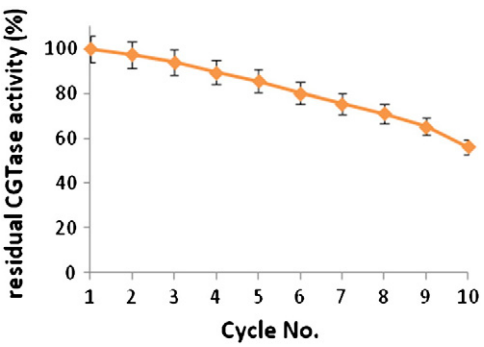

Fig. 12. Reusability of CGTase immobilized on mag@d-SiO_2@m-SiO_2-NH_2 nanospheres. Results represent the mean of three separate experiments, and error bars are indicated.

or lower pH, depending on surface charges and structure of the carrier (28,42) [24,41]. Similar behavior was reported by Song et al. [26] where optimal pH of immobilized superoxide dismutase was higher than free enzyme. However, the pH/activity profile of immobilized chitosanase was shifted toward acidic value [42]. For evaluation of the pH stability of CGTase, the free and immobilized enzyme was incubated for 3 h at varying pH values (pH 5.0 to 12.0) at room temperature. The results shown in Fig. 10b indicated that while free CGTase retained 77–87% of the initial enzyme activity at pH 6–10, immobilized CGTase retained 90–94%, indicating the significant enhancement of the pH stability of CGTase up on immobilization onto the activated amino functionalized magnetic double mesoporous core–shell silica nanospheres. This result is likely owing to the stabilization of the immobilized CGTase via multipoint attachment in the silica shell in addition to protection of the immobilized enzyme within the mesoporous silica shell nanopores [7].

3.4.2. Effect of temperature

The effect of temperature (30–70°C) on the catalytic activity of the free and immobilized CGTase is shown in Fig. 11a. The results indicated that the optimal temperature for the free CGTase activity was 50°C, whereas the optimal temperature for the immobilized enzyme was 50–55°C. In addition, the immobilized enzyme showed higher relative activities than free enzyme, particularly at high temperature (55–70°C). Investigation of the thermal stability demonstrated that the residual activity of the immobilized CGTase, after treatment at 60–70°C for 1 h, was higher than the free enzyme by about 1.1–1.1.9 fold (Fig. 11a), indicating significant improvement in the thermal stability of the CGTase up on immobilization on to the mag@d-SiO_2@m-SiO_2-NH_2. Enhancement of the thermal stability of the immobilized CGTase is probably due to covalent conjugation of the enzyme molecule within the mag@d-SiO_2@m-SiO_2-NH_2 nanospheres, which increase the rigidity of the enzyme three-dimensional structure and, hence, protect the immobilized CGTase against thermal denaturation [7,10,39].

3.4.3. Operational stability

The operational stability of the immobilized enzymes is one of the most important factors affecting the utilization of an immobilized enzyme system in industrial bioprocess. The results illustrated in Fig. 12 demonstrated that the immobilized CGTase could retain up to 86% and 56.3% of the initial activity after reutilizations for five and ten successive reactions, respectively; indicating that immobilized CGTase within mag@d-SiO_2@m-SiO_2-NH_2 nanospheres had good operational stability for industrial bioprocess.

4. Concluding remarks

Non-functionalized and functionalized magnetic double mesoporous core–shell silica nanospheres were successfully synthesized and characterized, and were first used as carriers for *Amphibacillus* sp. NPST-10 CGTase immobilization. Comparison of CGTase immobilization by physical adsorption and covalent attachment indicated that CGTase immobilization using covalent attachment onto the activated mag@d-SiO_2@m-SiO_2-NH_2 was the most effective and showed one of the highest immobilization yields and loading efficiencies reported so far for CGTase. In addition, the immobilized CGTase can be easily recovered using an external magnetic field. Immobilized CGTase showed significant improvement of thermal and pH of stability upon immobilization. Furthermore, the immobilized CGTase exhibited good operational stability, retaining 86% and 56.3% of the initial activity after reutilizations for five and ten successive reactions, respectively. The applied nano-structured carriers and immobilization protocol are promising approach for industrial bioprocess for production of cyclodextrins using immobilized CGTase.

Conflict of Interest

The authors whose names are listed immediately below certify that they have NO affi liations with or involvement in any organization or entity with any financial interest (such as honoraria; educational grants; participation in speakers' bureaus; membership, employment, consultancies, stock ownership, or other equity interest; and expert testimony or patent-licensing arrangements), or non-financial interest (such as personal or professional relationships, affiliations, knowledge or beliefs) in the subject matter or materials discussed in this manuscript.

Acknowledgments

This work was under financial supports of Strategic Technologies of the National Plan for Science and Technology, Saudi Arabia, through the project no. 11-BIO1480-02.

References

[1] Atanasova N, Kitayska T, Yankov D, Safarikova M, Tonkova A. Cyclodextrin glucanotransferase production by cell biocatalysts of alkaliphilic bacilli. Biochem Eng J 2009;46:278–85. http://dx.doi.org/10.1016/j.bej.2009.05.020.
[2] Svensson D, Adlercreutz P. Immobilization of CGTase for continuous production of long-carbohydrate-chain alkyl glycosides: Control of product distribution by flow rate adjustment. J Mol Catal B Enzym 2011;69:147–53. http://dx.doi.org/10.1016/j.molcatb.2011.01.009.
[3] Astray G, González-Barreiro C, Mejuto JC, Rial-Otero R, Simal-Gándara J. A review on the use of cyclodextrins in foods. Food Hydrocolloids 2009;23:1631–4. http://dx.doi.org/10.1016/j.foodhyd.2009.01.001.
[4] Moriwaki C, Ferreira LR, Rodella JRT, Matioli G. A novel cyclodextrin glycosyltransferase from *Bacillus sphaericus* strain 41: Production, characterization and catalytic properties. Biochem Eng J 2009;48:124–31. http://dx.doi.org/10.1016/j.bej.2009.09.001.
[5] Martin Del Valle EM. Cyclodextrins and their uses: A review. Process Biochem 2004;39:1033–46. http://dx.doi.org/10.1016/S0032-9592(03)00258-9.
[6] Otero-Espinar FJ, Luzardo-Álvarez A, Blanco-Méndez J. Cyclodextrins: More than pharmaceutical excipients. Mini Rev Med Chem 2010;10:715–25. http://dx.doi.org/10.2174/138955710791572479.
[7] Kim KD, Kim SS, Choa YH, Kim HT. Formation and surface modification of Fe_3O_4 nanoparticles by co-precipitation and sol–gel method. J Ind Eng Chem 2007;13:1137–41.
[8] Meunier CF, Dandoy P, Su BL. Encapsulation of cells within silica matrixes: Towards a new advance in the conception of living hybrid materials. J Colloid Interface Sci 2010;342:211–24. http://dx.doi.org/10.1016/j.jcis.2009.10.050.
[9] Leemhuis H, Kelly RM, Dijkhuizen L. Engineering of cyclodextrin glucanotransferases and the impact for biotechnological applications. Appl Microbiol Biotechnol 2010;85:823–35. http://dx.doi.org/10.1007/s00253-009-2221-3.
[10] Matte CR, Nunes MR, Benvenutti EV, Schoffer JN, Ayub MAZ, Hertz PF. Characterization of cyclodextrin glycosyltransferase immobilized on silica microspheres via aminopropyltrimethoxysilane as a "spacer arm". J Mol Catal B Enzym 2012;78:51–6. http://dx.doi.org/10.1016/j.molcatb.2012.01.003.
[11] Ansari SA, Husain Q. Potential applications of enzymes immobilized on/in nano materials: A review. Biotechnol Adv 2011;30:512–23. http://dx.doi.org/10.1016/j.biotechadv.2011.09.005.
[12] Kim J, Grate JW, Wang P. Nanostructures for enzyme stabilization. Chem Eng Sci 2006;61:1017–26. http://dx.doi.org/10.1016/j.ces.2005.05.067.
[13] Lee CH, Lin TS, Mou CY. Mesoporous materials for encapsulating enzymes. Nano Today 2009;4:165–79. http://dx.doi.org/10.1016/j.nantod.2009.02.001.
[14] Wang P. Nanoscale biocatalyst systems. Curr Opin Biotechnol 2006;17:574–9. http://dx.doi.org/10.1016/j.copbio.2006.10.009.
[15] Lei C, Soares TA, Shin Y, Liu J, Ackerman EJ. Enzyme specific activity in functionalized nanoporous supports. Nanotechnol 2008;19:125102. http://dx.doi.org/10.1088/0957-4484/19/12/125102.
[16] Serra E, Mayoral A, Sakamoto Y, Blanco RM, Díaz I. Immobilization of lipase in ordered mesoporous materials: Effect of textural and structural parameters. Microporous Mesoporous Mater 2008;114:201–13. http://dx.doi.org/10.1016/j.micromeso.2008.01.005.
[17] Deng H, Li X, Peng Q, Wang X, Chen J, Li Y. Monodisperse magnetic single-crystal ferrite microspheres. Angew Chem Int Ed 2005;44:2782–5. http://dx.doi.org/10.1002/anie.200462551.
[18] Ferrarotti SA, Bolivar JM, Mateo C, Wilson L, Guisan JM, Fernandez Lafuente R. Immobilization and stabilization of a cyclodextrin glycosyltransferase by covalent attachment on highly activated glyoxyl-agarose supports. Biotechnol Prog 2006;22:1140–5. http://dx.doi.org/10.1021/bp0600740.
[19] Ibrahim ASS, Al-Salamah AA, El-Tayeb MA, El-Badawi YB, Antranikian G. A novel cyclodextrin glycosyltransferase from Alkaliphilic *Amphibacillus* sp. NPST-10: Purification and properties. Int J Mol Sci 2012;13:10505–22. http://dx.doi.org/10.3390/ijms130810505.

[20] Cui Y, Li Y, Yang Y, Liu X, Lei L, Zhou L, et al. Facile synthesis of aminosilane modified superparamagnetic Fe_3O_4 nanoparticles and application for lipase immobilization. J Biotechnol 2010;150:171–4. http://dx.doi.org/10.1016/j.jbiotec.2010.07.013.
[21] Yiu HP, Wright PA, Botting NP. Enzyme immobilization using SBA-15 mesoporous molecular sieves with functionalized surfaces. J Mol Catal B Enzym 2001;15:81–92.
[22] Zhang L, Liu J, Yang J, Yang Q, Li C. Direct synthesis of highly ordered amine-functionalized mesoporous ethane-silicas. Microporous Mesoporous Mater 2008;109:172–83. http://dx.doi.org/10.1016/j.micromeso.2007.04.050.
[23] Nikolić MP, Giannakopoulos KP, Bokorov M, Srdić VV. Effect of surface functionalization on synthesis of mesoporous silica core/shell particles. Microporous Mesoporous Mater 2012;155:8–13. http://dx.doi.org/10.1016/j.micromeso.2011.12.046.
[24] Shi B, Wang Y, Ren J, Liu X, Zhang Y, Guo Y, et al. Superparamagnetic aminopropyl-functionalized silica core–shell microspheres as magnetically separable carriers for immobilization of penicillin G acylase. J Mol Catal B Enzym 2010;63:50–6. http://dx.doi.org/10.1016/j.molcatb.2009.12.003.
[25] Nabati F, Habibi-Rezaei M, Amanlou M, Moosavi-Movahedi AA. Dioxane enhanced immobilization of urease on alkyl modified nano-porous silica using reversible denaturation approach. J Mol Catal B Enzym 2011;70:17–22. http://dx.doi.org/10.1016/j.molcatb.2011.01.014.
[26] Song C, Sheng L, Zhang X. Preparation and characterization of a thermostable enzyme (Mn-SOD) immobilized on supermagnetic nanoparticles. Appl Microbiol Biotechnol 2012;96:123–32. http://dx.doi.org/10.1007/s00253-011-3835-9.
[27] Bradford MM. A rapid and sensitive method for the quantitation of microgram quantities of protein utilizing the principle of protein-dye binding. Anal Biochem 1976;72:248–54. http://dx.doi.org/10.1016/0003-2697(76)90527-3.
[28] Martin MT, Plou FJ, Alcalde M, Ballesteros A. Immobilization on Eupergit C of cyclodextrin glucosyltransferase (CGTase) and properties of the immobilized biocatalyst. J Mol Catal B Enzym 2003;21:299–308. http://dx.doi.org/10.1016/S1381-1177(02)00264-3.
[29] Gong J, Li S, Zhang D, Zhang X, Liu C, Tong Z. High quality self-assembly magnetite (Fe_3O_4) chain-like core-shell nanowires with luminescence synthesized by a facile one-pot hydrothermal process. Chem Commun 2010;46:3514–66. http://dx.doi.org/10.1039/C002199G.
[30] Mine E, Yamada A, Kobayashi Y, Konno M, Liz-Marzán LM. Direct coating of gold nanoparticles with silica by a seeded polymerization technique. J Colloid Interface Sci 2003;264:385–90. http://dx.doi.org/10.1016/S0021-9797(03)00422-3.
[31] Shu S, Zhang D, Chen Z, Zhang Y. Controlled synthesis of core/shell magnetic iron oxide/carbon systems via a self-template method. J Mater Chem 2009;19:7710–5. http://dx.doi.org/10.1039/B912057B.
[32] Bruce IJ, Sen T. Surface modification of magnetic nanoparticles with alkoxysilanes and their application in magnetic bioseparations. Langmuir 2005;21:7029–35. http://dx.doi.org/10.1021/la050553t.
[33] Yamaura M, Camilo RL, Sampaio LC, Macedo MA, Nakamura M, Toma HE. Preparation and characterization of (3-aminopropyl)triethoxysilane-coated magnetite nanoparticles. J Magn Magn Mater 2004;279:210–7. http://dx.doi.org/10.1016/j.jmmm.2004.01.094.
[34] Migneault I, Dartiguenave C, Bertrand MJ, Waldron KC. Glutaraldehyde: behaviour in aqueous solution, reaction with proteins, and application to enzyme crosslinking. Biotechniques 2004;37:790–6.
[35] Sulek F, Drofenik M, Habulin M, Knez Z. Surface functionalization of silica-coated magnetic nanoparticles for covalent attachment of cholesterol oxidase. J Magn Magn Mater 2010;322:179–85. http://dx.doi.org/10.1016/j.jmmm.2009.07.075.
[36] Sulek F, Knez Z, Habulin M. Immobilization of cholesterol oxidase to finely dispersed silica-coated maghemite nanoparticles based magnetic fluid. Appl Surf Sci 2010;256:4596–600. http://dx.doi.org/10.1016/j.apsusc.2010.02.055.
[37] Kong X, Chen Q. Experimental and theoretical investigations on the ferroelectricity of graphene oxides. Acta Chim Sin 2013;71:381–6. http://dx.doi.org/10.6023/A12090707.
[38] Jiang Y, Guo C, Xia H, Mahmood I, Liu C, Liu H. Magnetic nanoparticles supported ionic liquids for lipase immobilization: enzyme activity in catalyzing esterification. J Mol Catal B Enzym 2012;58:103–9. http://dx.doi.org/10.1016/j.molcatb.2008.12.001.
[39] Ranjbakhsh E, Bordbar AK, Abbasi M, Khosropour AR, Shams E. Enhancement of stability and catalytic activity of immobilized lipase on silica-coated modified magnetite nanoparticles. Chem Eng J 2012;179:272–6. http://dx.doi.org/10.1016/j.cej.2011.10.097.
[40] Xu XQ, Deng CH, Gao MX, Yu WJ, Yang PY, Zhang XM. Synthesis of magnetic microspheres with immobilized metal ions for enrichment and direct determination of phosphopeptides by matrix-assisted laser desorption ionization mass spectrometry. Adv Mater 2006;18:3289–93. http://dx.doi.org/10.1002/adma.200601546.
[41] Reshmi R, Sanjay G, Sugunan S. Enhanced activity and stability of α-amylase immobilized on alumina. Catal Commun 2006;7:460–5. http://dx.doi.org/10.1016/j.catcom.2006.01.001.
[42] Zeng J, Zheng LY. Studies on *Penicillium* sp. ZDZ1 chitosanase immobilized on chitin by cross-linking reaction. Process Biochem 2002;38:531–5. http://dx.doi.org/10.1016/S0032-9592(02)00163-2.